Atmos. Chem. Phys. Discuss., 9, 12007–12025, 2009
www.atmos-chem-phys-discuss.net/9/12007/2009/

Atmospheric Chemistry and Physics Discussions

This discussion paper is/has been under review for the journal *Atmospheric Chemistry and Physics (ACP)*. Please refer to the corresponding final paper in *ACP* if available.

Direct measurements of the effect of biomass burning over the Amazon on the atmospheric temperature profile

A. Davidi[1], **I. Koren**[1], **and L. Remer**[2]

[1]Department of Environmental Sciences, Weizmann Institute, Rehovot, Israel
[2]NASA Goddard Space Flight Center, Greenbelt, Maryland, USA

Received: 6 April 2009 – Accepted: 12 May 2009 – Published: 15 May 2009

Correspondence to: A. Davidi (amit.davidi@weizmann.ac.il)

Published by Copernicus Publications on behalf of the European Geosciences Union.

Abstract

Aerosols suspended in the atmosphere interact with the solar radiation and thus change the radiation energy fluxes in the atmospheric column. In particular, absorbing aerosols can stabilize the lower atmosphere by warming the aerosol layer; while cooling both: the layers beneath and the surface. Changes in atmospheric stability can affect cloud formation and cloud properties. In this paper we measure changes in the atmospheric temperature profile as a function of the smoke loading and the cloudiness over the Amazon basin, during the dry seasons (August and September) of 2005–2007. We show that as the aerosol optical depth (AOD) increases from 0.02 to a value of ~0.6, there is a decrease of ~4.3°C at 1000 hPa, and an increase of ~1.6°C at 850 hPa. The warming of the aerosol layer at 850 hPa is likely due to aerosol absorption when the particles are exposed to direct illumination by the sun. The large values of cooling in the lower layers are explained by a combination of aerosol extinction of the solar flux in the layers aloft and by an aerosol-induced increase of cloud cover and further shading of the lower atmosphere. We estimate that the increase in cloud fraction due to aerosol contributes about half of the observed cooling in the lower layers.

1 Introduction

Aerosol effects on clouds contribute the largest uncertainties in estimating the anthropogenic role in climate change (IPCC, 2007). Aerosols can affect cloud properties through two separate pathways, the microphysical and the radiative (Kaufman and Koren, 2006; Koren et al, 2008). The first pathway follows aerosol-induced changes to the cloud condensation nuclei (CCN) and ice nuclei (IN) concentrations and distributions, thus changing the microphysical properties of the cloud, and igniting a series of feedbacks (Twomey, 1977; Rosenfeld, 2000; Koren et al, 2005). The second pathway originates in the optical properties of the aerosols. Aerosols scatter and absorb solar radiation (Hansen et al., 1997; Ackerman et al., 2000), thus reducing the amount of ra-

ACPD

9, 12007–12025, 2009

diation reaching the ground, which cools the surface. This affects the energy balance of the surface, decreasing surface latent and sensible heat fluxes, which inhibits cloud formation. In addition, by absorbing solar radiation, biomass burning aerosols heat the atmospheric layer in which they are located. Warming the layer reduces cloudiness due to: (i) reduction of local relative humidity; (ii) creating a more stable atmosphere and producing less convection; therefore, a cooler surface and more stable atmosphere may (iii) reduce fluxes of moisture from the surface (evaporation and evapotranspiration) to the atmosphere (Koren et al., 2004; Feingold et al., 2005). The last process is of great importance in the Amazonian atmosphere, where ~50% of the available atmospheric moisture comes from evapotranspiration of the canopy (Salati, 1987).

The two pathway conceptual model is supported by observational evidence that shows the relationship between cloud properties and aerosol loading (Koren et al., 2008). Furthermore, a large body of observational evidence supports the fundamentals of the microphysical pathway (Jiang and Feingold, 2006; Andreae and Rosenfeld, 2008). However, the fundamentals of the second pathway, that aerosols are heating the atmosphere and cooling the surface, are based on radiative transfer calculations. There have been no direct measurements, that the authors aware of, of aerosol heating or cooling the atmospheric column, on a regional and seasonal basis.

In this paper we directly measure the change in atmospheric temperature profile over the Amazon basin due to the presence of absorbing aerosols emitted from biomass burning during the dry seasons (August and September) of 2005–2007.

The atmospheric temperature profile is measured with the Atmospheric Infra-Red Sounder (AIRS), on Aqua (Aumann et al., 2003). AIRS has been validated over all geophysical conditions: polar, non-polar, day, night, land and ocean (Olsen et al., 2007). In particular, AIRS has been validated over the Amazon basin (Souza et al., 2005). An important issue is how cloudy skies affect the AIRS temperature profile retrieval. Tobin et al. (2006) studied the AIRS retrieval in 2 ARM (Atmospheric Radiation Measurement) sites: north central Oklahoma (97.5° W, 36.6° N) and tropical western Pacific (166.9° E, 0.5° S), compared with dedicated radiosondes. He showed that biases and variations

ACPD
9, 12007–12025, 2009

in the temperature profiles do not correlate significantly with cloud fraction. In addition, Reale et al. (2008) showed that forecasts can be improved by assimilation of AIRS temperature retrievals under cloudy conditions; this further supports the validity of the retrieval.

2 Methodology

The analyzed region over the Amazon basin was chosen to include the most polluted areas, while staying in a relatively small region (see Fig. 1) the area encompasses $\sim 2 \times 106\,km^2$. Also, to take advantage of the stable synoptic high pressure system (Nobre et al., 1998) without the complications of local geographically induced circulations, care was taken to not include the Andes and to be sufficiently far from the seashores.

We focus on the peak of the biomass burning season, August and September, for the years 2005–2007. Aerosol optical depth (AOD) data were taken from the MODerate resolution Imaging Spectroradiometer (MODIS) retrievals (Remer et al., 2008; Levy et al., 2007). We use Collection 5, Level 3, 1-degree, daily data; and unless otherwise specified all AOD is at 550 nm. Atmospheric temperature profiles are retrieved from the Atmospheric Infra-Red Sounder (AIRS) (Aumann et al., 2003). We use Daily Global Level 3 products (1-degree resolution). Both MODIS and AIRS fly on the Aqua platform (~01:30 p.m. local time). In addition, we use total attenuated backscatter (at 532 nm) images from Cloud-Aerosol Lidar with Orthogonal Polarization (CALIOP), on Calipso, in order to estimate the smoke layer height (Winker et al., 2003).

We have analyzed the AIRS retrieved temperatures at 4 altitude levels: 1000, 925, 850, and 700 hPa. Since the horizontal temperature gradients at each altitude are expected to be smooth in our region of interest, we screen out outliers which show sharp changes of temperature relative to their neighbours (thus eliminating less than 3% of the data). The data were sorted according to AOD and binned into ~25 bins with equal number of samples in each bin to maintain similar temperature variances. A scatter plot of the mean temperature of each bin versus the mean AOD of each bin

ACPD
9, 12007–12025, 2009

was plotted. An estimation of the error was calculated from the standard error of the mean in each bin. To minimize cloud contamination, the AOD values were restricted to 0.6 and below (Brennan et al., 2005).

To reduce the variance in temperature T due to daily meteorological differences and to focus on the regional aerosol effect on the profile we looked first on the correlations between the differences in the local temperature less the daily average for the region (defined as "delta temperature") $\Delta T \equiv T - <T>_{\text{daily}}$, against the aerosol optical depth (AOD). The ΔT versus AOD plot will show the functional relationship between temperature and aerosol, even if there are day to day variations in regional temperature at any atmospheric layer. However the correlations between ΔT to AOD and the T to AOD (without the subtraction of the daily average) were almost identical suggesting that the daily variances of the temperatures due to meteorological conditions are small. Figure 2 shows the correlations between the absolute temperature T (blue) and the delta temperature ΔT (magenta) for the lowest pressure level (1000 hPa). Other altitudes showed similar results. Because no significant difference is observed, further analysis is done with T (the absolute temperature).

3 Results

Figure 3 shows the binned scatter plot of the temperature versus AOD of the 4 altitudes. As AOD increases from the lowest average value of 0.02 to 0.6, there is a decrease of ~4.3°C at 1000 hPa (blue curve); a decrease of ~1.9°C at 925 hPa (green), an increase of ~1.6°C at 850 hPa (red); and no significant change at 700 hPa (cyan). The difference between the curves at 1000 and 850 hPa can serve as a good measure for the stability of the lower atmosphere. The temperature difference between 1000 to 850 hPa (~1500 m) along the dry adiabatic lapse-rate is ~15°C (Rogers and Yau, 1980). While the average temperature difference is 18.4°C for the clean atmosphere (AOD=0.02, solid arrow, Fig. 3) suggesting non stable atmosphere, the average temperature difference for the polluted cases (AOD=0.5, dashed arrow, Fig. 3) is only 12.5°C indicating a

ACPD
9, 12007–12025, 2009

clear shift toward stable atmosphere. Thus, higher values of AOD are associated with a more stable atmosphere at 850 hPa and below as seen visually by the convergence of the curves at 1000 and 850 hPa.

What portion of the temperature change is directly due to the interaction of the smoke with the solar radiation and what is the contribution of the feedback of the smoke changes of the cloudiness? It was shown in Koren et al. (2008) that the cloud fraction (the portion of the sky that is covered by clouds) correlates logarithmically with the aerosols optical depth (AOD). These correlations are driven by the microphysical effects of aerosols on clouds. When there are few aerosol particles and AOD is low, small changes in the number of aerosols acting as cloud condensation nuclei (CCN) or ice nuclei (IN) can dramatically change the cloud properties (fraction, vertical development, reflectivity). However, the microphysical effects tend to saturate, meaning that additional particles will not change the cloud properties in cases where the CCN concentrations are high ($\sim$1000 per cm^3). The saturation of the microphysical effect was shown to occur at AOD$\sim$0.3 for the Amazonian smoke (Koren et al., 2008).

Both aerosol direct heating/cooling and indirect heating/cooling from aerosol-induced changes to cloud cover are inherently bundled together into Fig. 3. In order to differentiate between aerosol direct heating/cooling of the atmosphere from aerosol-induced cloud cover effects, we repeated Fig. 3, but divided the data into two classes according to the cloud cover (CC) values: low cloud cover (CC<0.3) and high cloud cover (CC>0.3); Fig. 4a and b, respectively.

In low cloud cover (CC) skies (CC<0.3, Fig. 4a), we see a rise in temperature at 850 hPa similar to that in Fig. 3; however, at 1000 hPa the temperature decrease is reduced to $\sim$2.5°C, compared with $\sim$5°C in Fig. 3. In high cloud cover (CC>0.3, Fig. 4b), the overall pattern is similar to the low CC case, but at 1000 hPa (blue) we see a rapid decrease of $\sim$6°C as the AOD values reaches $\sim$0.3, and then a very mild increase (although not significant with respect to the error-bars) of the temperature as AOD values rise. In addition, at 850 hPa (red curve, Fig. 4b) we see a linear increase of the temperature until AOD values reach $\sim$0.35, and then no significant change. A plot of

ACPD
9, 12007–12025, 2009

clear skies only (i.e. CC=0) was not possible due to the scarcity of the data. In order to verify the microphysical effect of the aerosols, we plot the change in the cloud cover as a function of AOD for the two data groups. In low cloud covers (Fig. 4c), the AOD has a mild effect on the cloud cover, while in the high cloud cover (Fig. 4d) we see a sharp increase in cloud cover as AOD reaches a value of ∼0.3 and then a mild decrease (again, not significant with respect to the error-bars).

To further explore whether the apparent aerosol-induced changes to the temperature profile are related to the direct/heating cooling of the aerosol particles, we need to confirm whether the aerosol layer corresponds to the altitudes where we see the temperature profile change. CALIPSO backscatter data were used (Thomason et al, 2007) to estimate the smoke layer altitude. Figure 5a shows a characteristic CALIPSO total attenuated backscatter at 532 nm image over the Amazon basin (from date: 17/8/2007, time: 17:24:18). We distinguish smoke from cloud by the fact that smoke is more homogeneous and with lower optical density compared with clouds. A true color image from MODIS is shown in Fig. 5b, which helps identify smoke and clouds in the CALIPSO image. The smoke layer extends from the ground to an altitude of about 3.3 km. Examination of 16 CALIPSO images distributed over the 2 month period shows that the smoke reaches an altitude of 3.4±0.2 km. However, CALIPSO does not provide the distribution of the smoke concentration within the layer. Atmospheric sounding data (http://weather.uwyo.edu/upperair/sounding.html) at the Manaus station in the Amazon (station number 82 332), translates the AIRS pressure levels of 1000, 925, 850, and 700 hPa to altitudes of ∼110 m, ∼800 m, ∼1500 m, and ∼3200 m, respectively. The combination of the CALIPSO lidar and Manaus sounding data indicate that the four AIRS pressure levels of Figs. 3 and 4 fall within the observed layer, with the 700 hPa at the very top of the smoke.

ACPD
9, 12007–12025, 2009

4 Discussion

Figures 3 and 4 present a compelling association between increasing aerosol optical depth in the Amazon and measurable temperature changes within the lower atmosphere. While the altitudes exhibiting the temperature changes lie within the characteristic smoke layer, as observed by CALIPSO, the temperature changes cannot be due solely to heating/cooling by the aerosol absorption and scattering. For one, the magnitudes of the low altitude temperature changes associated with increasing AOD are larger than expected from aerosol absorption alone (Koren et al., 2004). By controlling for cloud cover, we see that both the magnitude of the cooling of the lowest layers decreases; and saturation appears at AOD~0.3 for high cloud covers, which agrees with the saturation of the cloud cover at AOD above ~0.3 (Fig. 4d). Therefore, we conclude that the temperature changes associated with increasing AOD in the Amazon biomass burning season is a combination of aerosol direct heating/cooling and aerosol-induced changes to cloud cover that results in additional low altitude cooling and a characteristic "saturation" at AOD~0.3.

Specifically, the temperature rise at 850 hPa is primarily a result of the absorption of solar radiation by the biomass burning aerosols at this level. The magnitudes are consistent with expectations and there is a steady rise in temperature as AOD increases. However, this absorption is cloud dependent by the fact that in cloudy skies less radiation reaches the aerosols and thus the heating is diminished, according to the Absorption Fraction Feedback (Koren et al, 2008). Indeed there is less heating in this layer in the data subset with the high cloud cover (Fig. 4b). However, the temperature decrease near the surface (1000 hPa pressure level) is due to the absorption and scattering of solar radiation by the smoke above, combined with cooling by cloud shading. When we restrict the cloud cover to a narrow range, minimizing the cloud contribution, we see significant differences in the temperature versus AOD plots than when we allow unrestricted cloud covers. Most importantly with restricted cloud cover ranges, the cooling associated with increased AOD is cut in about half and the temperature decrease is a

ACPD
9, 12007–12025, 2009

linear function of AOD with no saturation point.

The saturation point at AOD∼0.3 for high cloud cover (Fig. 4b) corresponds to the point at which the aerosol effects on cloud cover switch from primarily the microphysical pathway to the radiative pathway (Koren et al., 2008). In a very pristine atmosphere, addition of aerosol in the form of cloud condensation nuclei (CCN) introduces substantial changes to the cloud microphysics. More numerous but smaller droplets form, and this affects cloud extent and lifetime. The result is a rapid increase of cloud cover as AOD increases from near zero to around 0.3. At that point the microphysical pathway reaches a saturation point. Additional CCN do not further increase cloud cover, and instead the radiative pathway becomes dominant.

In the unrestricted analysis (all data, Fig. 3) we see the combination of both processes. As the atmosphere transitions from a clean pristine environment to a moderately smoky one, the smoke heats the atmospheric layer at 850 hPa, but also rapidly increases cloud cover, shading the 1000 hPa layer and cooling it. Once the AOD values surpass moderate levels, cloud cover no longer increases and the cooling effect of the increased cloud shading is somewhat diminished. Meanwhile, the 850 hPa layer continues its steady temperature increase.

The pressure level 925 hPa can be viewed as a transition altitude. It is affected similarly to the lower atmospheric level of 1000 hPa, but at weaker magnitudes. Meanwhile the 700 hPa level is at the very top of the smoke layer where the smoke is thinly concentrated, and therefore does not respond to increasing smoke in the layers beneath.

The relationship between temperature and AOD of the 4 pressure levels taken as a whole shows clearly the stabilizing effect of the smoke on the lower atmosphere. The temperature difference between the lowest atmospheric layer at 1000 hPa and the 850 hPa layer (∼1500 m), $\Delta T = T(1000\,\text{hPa}) - T(850\,\text{hPa})$, can serve as an indication of the stability of the atmosphere. The dry adiabatic lapse rate is about -1°C per 100 m (Rogers and Yau, 1989); and therefore, yields a decrease of $\sim 15^{\circ}$C for the height differences between the 1000 hPa and 850 hPa levels. Figure 3 shows that for the clean atmosphere (AOD<0.1) $\Delta T \sim 18.4^{\circ}$C suggesting an unstable atmosphere, but for

ACPD
9, 12007–12025, 2009

the more smoky situations (AOD>0.5) $\Delta T \sim 12.5^{\circ}$C, suggesting a transition to a stable atmosphere. This stabilization is partly due to the direct interaction of the smoke with the solar radiation and partly due to the feedback in which smoke increases cloud cover. Thus, the microphysical pathway in which aerosol particles increase cloud cover is self-limiting: more clouds lead to a more stable atmosphere, which will eventually reduce cloudiness.

We have done the same analysis also for the years 2005 and 2006. Table 1 summarizes the results for all the years for unrestricted cloud cover (i.e. for 2007, the numbers correspond to Fig. 3). Small differences are expected due to interannual variation in meteorological conditions and biomass burning policies. The response to cloud cover restrictions is the same for 2005 and 2006, as it was for 2007 and shown in Fig. 4.

In this paper we showed – for the first time using observations – the dependence of the Amazonian atmospheric temperature profile on AOD and the effect of cloud cover on this dependence. The direct interaction of the smoke with the solar radiation and the "smoke-increasing cloud fraction" feedback are coupled and both affect the temperature profile. To decouple these processes, as a first approximation we restricted the data to two cloud cover ranges. By restricting cloud cover, the variance can be more easily assigned to each of the two pathways: the microphysical and the radiative. However, it must be acknowledged that the microphysical effect is not completely eliminated, and some of the trends shown in the restricted subsets can be due to the aerosol effect on clouds. Moreover, in addition to the coupling between clouds, aerosol and radiation demonstrated here, the relationships between atmospheric temperature profile and AOD also include components that link atmospheric temperature responses to surface and biospheric processes, and to large-scale meteorology. Illustration of the more complicated picture requires tools beyond those employed in this study.

Acknowledgements. This paper is dedicated to the memory of Yoram J. Kaufman, a dear friend and a brilliant scientist. This research was supported by the Israel Science Foundation (grant no. 1355/06), the Minerva Foundation and NASA's Interdisciplinary Science Program under the direction of H. Maring. I. K. is the incumbent of the Benjamin H. Swig and Jack D. Weiler career

development chair at the Weizmann Institute.

References

Ackerman, A. S., Toon, O. B., Stevens, D. E., Heymsfield, A. J., Ramanathan, V., and Welton, E. J.: Reduction of tropical cloudiness by soot, Science, 288, 1042–1047, 2000.

Andreae, M. O. and Rosenfeld, D.: Aerosol-cloud-precipitation interactions. Part 1. The nature and sources of cloud-active aerosols, Earth Sci. Rev., 89, 13–41, 2008.

Aumann, H. H., Chahine, M. T., Gautier, C., Goldberg, M. D., Kalnay, E., McMillin, L. M., Revercomb H., Rosenkranz, P. W., Smith, W. L., Staelin, D. H., Strow, L. L., and Susskind , J.: AIRS/AMSU/HSB on the Aqua mission: Design, science objectives, data products, and processing systems, IEEE Trans. Geosci. Remote Sens., 41(2), 253–264, 2003.

Brennan, J. I., Kaufman, Y. J., Koren, I., and Li, R. R.: Aerosol-cloud interaction – misclassification of MODIS clouds in heavy aerosol, IEEE Trans. Geosci. Remote Sens., 43(4), 911–915, 2005.

Feingold, G., Jiang, H., and Harrington, J. Y.: On smoke suppression of clouds in Amazonia, J. Geophys. Res., 32, L02804, doi:10.1029/2004GL021369, 2005

Hansen, J., Sato, M., and Ruedy, R.: Radiative forcing and climate response, J. Geophys. Res., 102, 6831–6864, 1997.

IPCC: The Intergovernmental Panel on Climate Change (IPCC), Working Group I Report "The Physical Science Basis", http://www.ipcc.ch/pdf/assessment-report/ar4/wg1/ar4-wg1-chapter2.pdf, (last access: 21 July 2008), 2007.

Jiang, H. and Feingold, G.: Effect of aerosol on warm convective clouds: Aerosol-cloud-surface flux feedbacks in a new coupled large eddy model, J. Geophys. Res., 111, D01202, doi:10.1029/2005JD006135, 2006.

Kaufman, Y. J. and Koren, I.: Smoke and pollution aerosol effect on cloud cover, Science, 313, 355–658, 2006.

Koren, I., Kaufman, Y. J., Remer, L. A., and Martins, J. V.: Measurement of the effect of Amazon smoke on inhibition of cloud formation, Science, 303, 1342–1345, 2004.

Koren, I., Kaufman, Y. J., Resonfeld, D., Remer, L. A., and Rudich, Y.: Aerosol invigoration and restructuring of Alantic convctive clouds, Geophys. Res. Lett., 32, L14828, doi:10.1029/2005GL023187, 2005.

Koren, I., Martins, J. V., Remer, L. A., and Afargan, H.: Smoke invigoration versus inhibition of clouds over the Amazon, Science, 321, 946–949, 2008.

Levy, R. C., Remer, L. A., Mattoo, S., Vermote, E. F., and Kaufman, Y. J.: Second-generation operational algorithm: Retrieval of aerosol properties over land from inversion of Moderate Resolution Imaging Spectroradiometer spectral reflectance, J. Geophys. Res., 112, D13211, doi:10.1029/2006JD007811, 2007.

Nobre, C. A., Mattos, L. F., Dereczynski, C.P., Teresova, T. A., and Trosnikov, I. V.: Overview of atmospheric conditions during the Smoke, Clouds, and Radiation–Brazil (SCAR-B) field experiment, J. Geophys. Res., 103, 31809–31820, 1998.

Olsen, E. T., Fetzer, E., Lee, S-Y, Manning, E., Blaisdell, J., and Susskind, J.: AIRS/AMSU/HSB version 5 CalVal status summary, available at: http://disc.gsfc.nasa.gov/AIRS/documentation, 2007.

Reale, O., Susskind, J., Rosenberg, R., Brin, E., Liu, E., Riishojgaard, L. P., Terry, J., and Jusem, J. C.: Improving forecast skill by assimilation of quality-controlled AIRS temperature retrievals under partially cloudy conditions, Geophys. Res. Lett., 35, L08809, doi:10.1029/2007GL03302, 2008.

Remer, L. A., Kleidman, R. G., Levy, R. C., Kaufman, Y. J., Tanre, D., Mattoo, S., Martins, J. V., Ichoku, C., Koren, I., Yu, H., and Holben, B. N.: Global aerosol climatology from the MODIS satellite sensors, J. Geophys. Res., 113, D14S07, doi:10.1029/2007JD009661, 2008.

Rogers, R. R. and Yau, M. K.: A Short Course in Cloud Physics, 3rd ed., pp. 28-29, Elsevier Science, Massachusetts, 1989.

Rosenfeld, D.: Suppression of rain and snow by urban and industrial air pollution, Science, 287, 1793–1796, 2000.

Salati, E.: The forest and the hydrological cycle, in: , Geophysiology of Amazonia, edited by: Dickinson, R. E., John Wiley & Sons, New York, 273–296, 1987.

Souza, R. A. F., Ceballos, J. C., and Barnet, C. D.: Performance of the AQUA/NASA and NOAA-16/ICI soundings over Rondonia during the Dry-To-Wet LBA experiment, Proceedings of The Fourteenth International TOVS Study Conference, 25–31 May, Beijing, China, 2005.

Tobin, D. C., Revercomb, H. E., Knuteson, R. O., Lesht, B. M., Strow, L. L., Hannon, S. E., Feltz, W. F., Moy, L. A., Fetzer, E. J., and Cress, T. S.: Atmospheric Radiation Measurement site atmospheric state best estimates for Atmospheric Infrared Sounder temperature and water vapor retrieval validation, J. Geophys. Res., 111, D09S14, doi:10.1029/2005JD006103, 2006.

Thomason, L. W., Pitts, M. C., and Winker, D. M.: CALIPSO observations of stratospheric aerosols: a preliminary assessment, Atmos. Chem. Phys., 7, 5283–5290, 2007, http://www.atmos-chem-phys.net/7/5283/2007/.

Twomey, S.: The influence of pollution on the shortwave albedo of clouds, J. Atmos. Sci., 34, 1149–1152, 1977.

Winker, D. M., Pelon, J., and McCormick, M. P.: The CALIPSO mission: Space borne lidar for observation of aerosols and clouds, Proc. SPIE, 4893, 1–11, 2003.

Table 1. A summary for the years 2005–2007.

Year	ΔT [°C]	
	1000 hPa	850 hPa
2005	−6±1	2.3±0.5
2006	−6.8±0.9	1±0.3
2007	−4.3±0.8	1.6±0.3

ACPD

9, 12007–12025, 2009

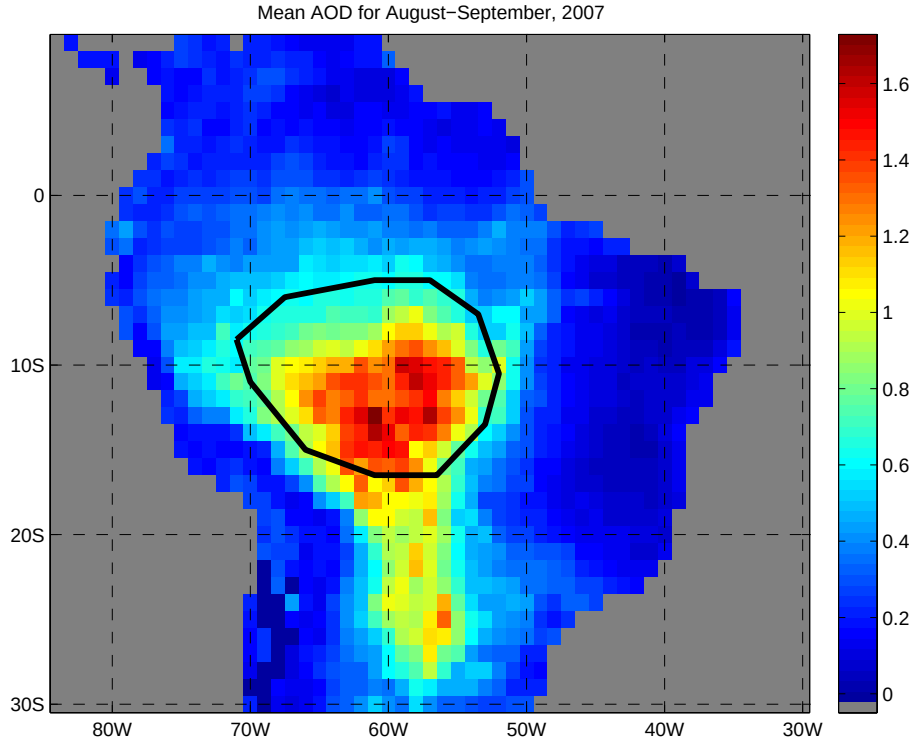

Fig. 1. Topographic image of the region of interest (ROI) – black line. The ROI encompasses $\sim 2 \times 10^6$ km^2.

ACPD

9, 12007–12025, 2009

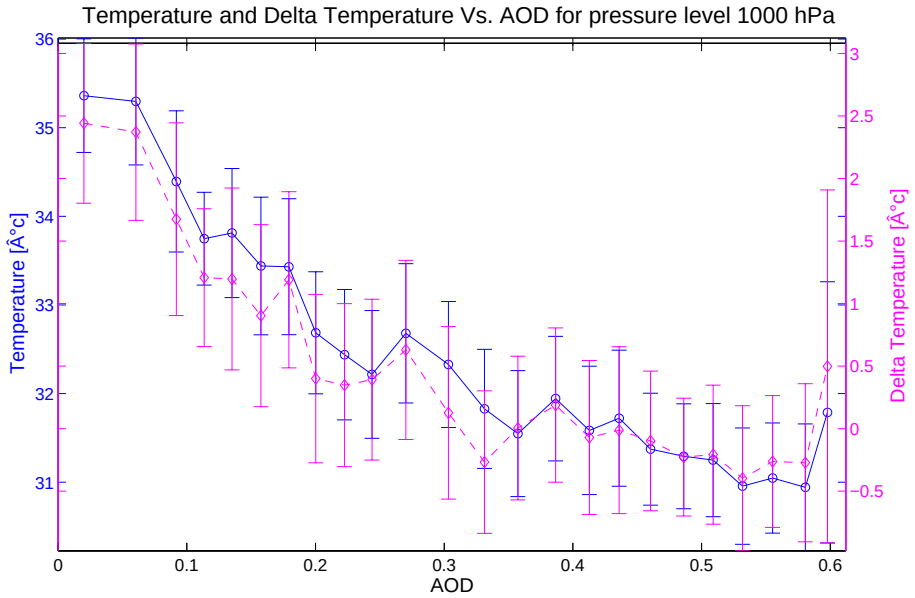

Fig. 2. Scatter plots of temperature (blue) and "delta temperature" (magenta) vs. AOD, for the 1000 hPa level. "Delta temperature" is the difference in the local temperature less the daily average for the region.

ACPD
9, 12007–12025, 2009

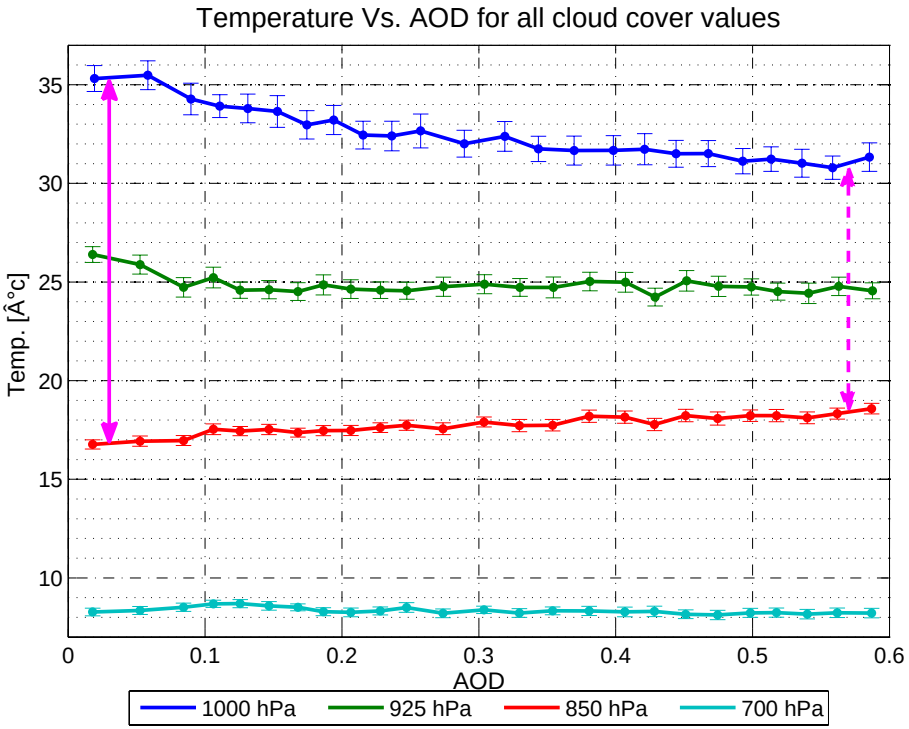

Fig. 3. Temperature vs. AOD, for all cloud covers, at four different levels of the atmosphere: 1000 hPa (blue), 925 hPa (green), 850 hPa (red), and 700 hPa (cyan). Each point represents a mean temperature for a particular AOD bin, and error bars are the standard error of the mean in the bin. The data consists of AIRS temperature profiles collocated with MODIS retrievals of AOD, on a daily 1-degree grid.

ACPD
9, 12007–12025, 2009

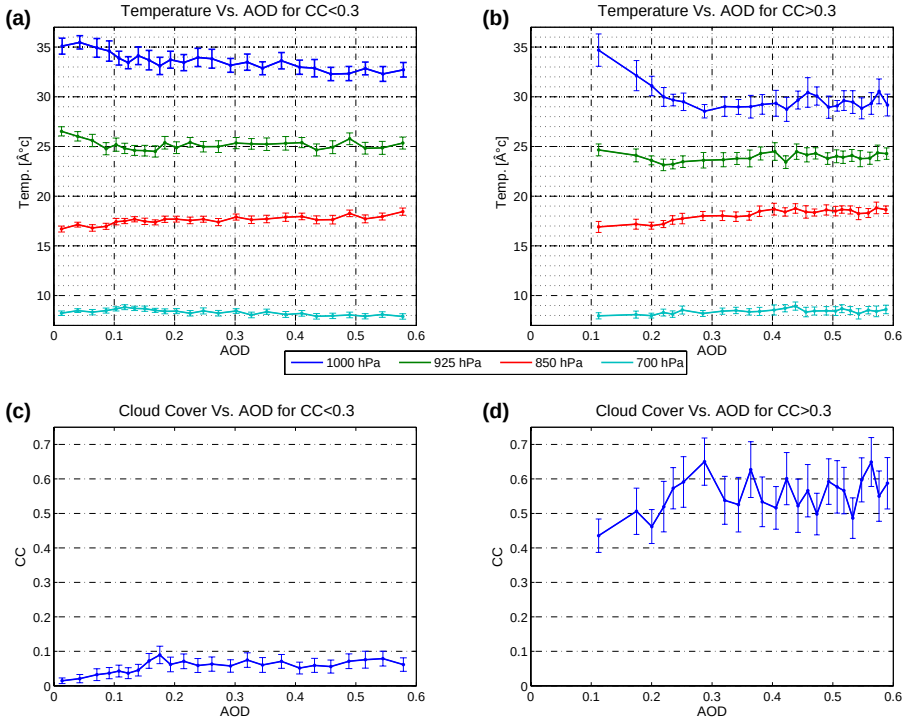

Fig. 4. **(a)** The same as Fig. 3, but for CC (cloud cover) below 0.3; **(b)** for CC above 0.3; **(c)** change in CC as a function of AOD, for CC<0.3; **(d)** change in CC as a function of AOD, for CC>0.3.

ACPD
9, 12007–12025, 2009

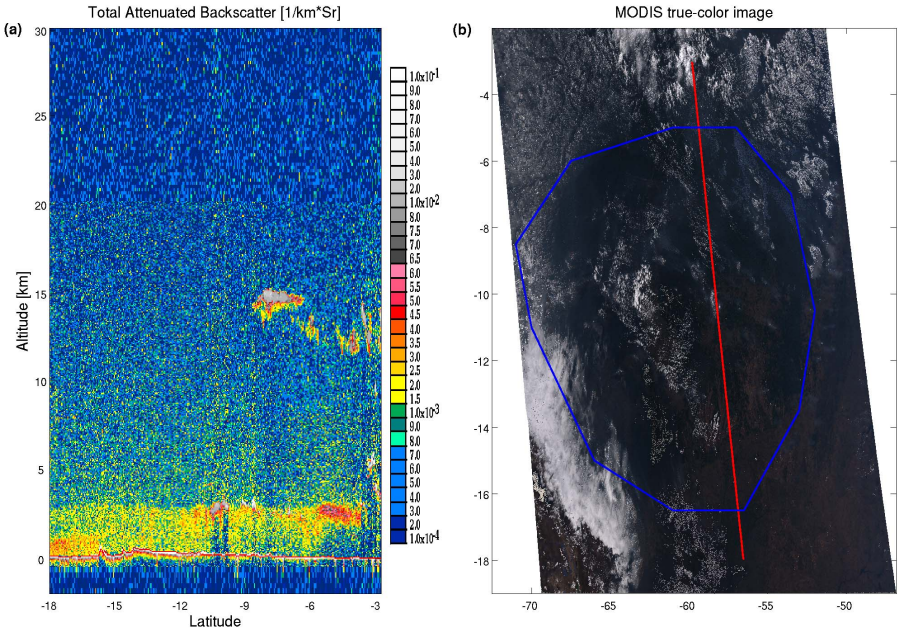

Fig. 5. (a) – Calipso image of total attenuated backscatter at 532 nm (date: 17/8/2007, time: 17:24:18); **(b)** – True color image from MODIS on Aqua, red – Calipso's route, blue – region studied (see Fig. 1).

ACPD

9, 12007–12025, 2009